

Rohan J. Hudson, David M. Huang and Tak W. Kee

Anisotropic triplet exciton diffusion in crystalline functionalized pentacene

The Journal of Physical Chemistry C, 2020; 124(43):23541-23550

This document is the Accepted Manuscript version of a Published Work that appeared in final form in The Journal of Physical Chemistry C, copyright © 2020 American Chemical Society after peer review and technical editing by the publisher. To access the final edited and published work see <http://dx.doi.org/10.1021/acs.jpcc.0c07608>

PERMISSIONS

https://pubs.acs.org/page/copyright/journals/posting_policies.html#policies-7

7. Posting Accepted and Published Works on Websites and Repositories: A digital file of the Accepted Work and/or the Published Work may be made publicly available on websites or repositories (e.g. the Author's personal website, preprint servers, university networks or primary employer's institutional websites, third party institutional or subject-based repositories, conference websites that feature presentations by the Author(s) based on the Accepted and/or the Published Work), and on Private Research Collaboration Groups under the following conditions:

- It is mandated by the Author(s)' funding agency, primary employer, or, in the case of Author(s) employed in academia, university administration.
- If the mandated public availability of the Accepted Manuscript is sooner than 12 months after online publication of the Published Work, a waiver from the relevant institutional policy should be sought. If a waiver cannot be obtained, the Author(s) may sponsor the immediate availability of the final Published Work through participation in the ACS AuthorChoice program—for information about this program see [ACS Open Access Licensing Options](#).
- If the mandated public availability of the Accepted Manuscript is not sooner than 12 months after online publication of the Published Work, the Accepted Manuscript may be posted to the mandated website or repository. The following notice should be included at the time of posting, or the posting amended as appropriate: "This document is the Accepted Manuscript version of a Published Work that appeared in final form in [Journal Title], copyright © American Chemical Society after peer review and technical editing by the publisher. To access the final edited and published work see [insert ACS Articles on Request author-directed link to Published Work, see [ACS Articles on Request](#)]."
- The posting must be for non-commercial purposes and not violate the ACS' "[Ethical Guidelines to Publication of Chemical Research](#)", although posting in Private Research Collaboration Groups on commercially-operated Scientific Collaboration Networks that are signatories to the [STM Voluntary Principles](#) is permissible.
- Regardless of any mandated public availability date of a digital file of the final Published Work, Author(s) may make this file available only via the ACS AuthorChoice Program. For more information, see [ACS Open Access Licensing Options](#)

Author(s) may post links to the Accepted Work on the appropriate ACS journal website if the journal posts such works. Author(s) may post links to the Published Work on the appropriate ACS journal website using the [ACS Articles on Request author-directed link](#).

Links to the Accepted or Published Work may be posted on the Author's personal website, university networks or primary employer's institutional websites, and conference websites that feature presentations by the Author(s). Such posting must be for non-commercial purposes.

14 November 2023

<http://hdl.handle.net/2440/129896>

Anisotropic Triplet Exciton Diffusion in Crystalline Functionalized Pentacene

Rohan J. Hudson, David M. Huang,* and Tak W. Kee*

*Department of Chemistry, The University of Adelaide, Adelaide, South Australia, 5005,
Australia*

E-mail: david.huang@adelaide.edu.au; tak.kee@adelaide.edu.au

Phone: +61-(0)8-8313-5580; +61-(0)8-8313-5314

Abstract

Exciton multiplication through singlet fission (SF) offers scope for next-generation photovoltaic devices to exceed the Shockley-Queisser limit. Organic SF chromophores typically exhibit significant structural anisotropy in their crystal packing, which can impact exciton transport and influence the design of SF-enhanced devices. An improved understanding of the link between structural anisotropy and exciton diffusion is therefore crucial for developing SF-based photovoltaics. Here, we use femtosecond transient absorption spectroscopy to quantify the anisotropic triplet mobility in 6,13-(triisopropylsilylethynyl)pentacene (TIPS-Pn), a prototypical SF chromophore. Bimolecular triplet-triplet annihilation (TTA) in crystalline TIPS-Pn is well-described by a kinetic model that assumes isotropic, three-dimensional triplet exciton diffusion, but with best-fit parameters that do not correspond to any physical parameters of the material. Kinetic models that assume either one-dimensional or anisotropic three-dimensional exciton diffusion describe the annihilation equally well but yield more physically realistic fit parameters, suggesting that triplet diffusion on the sub-nanosecond timescale occurs mostly along a single axis of the material. These findings highlight the need to treat parameters obtained from fits of experimental data with models of isotropic diffusion with caution for systems with anisotropic packing such as TIPS-Pn. Diffusion coefficients calculated by density functional theory predict that triplet exciton diffusion occurs predominantly along the crystallographic a -axis, with migration in any other direction through the crystal slower by over an order of magnitude. This anisotropic diffusion suggests that fast, directional exciton transport in layers or films of TIPS-Pn may be achieved by control of the chromophore morphology.

Introduction

Singlet exciton fission (SF) is the photophysical process in which a chromophore in a singlet excited state couples to an adjacent ground state chromophore to yield two triplet excited state chromophores.¹ SF has garnered significant interest in recent years, as it may help to surpass the Shockley–Queisser limit of single-junction photovoltaic (PV) devices.^{2,3} However, practical implementations of SF-sensitized PV devices have shown only minor efficiency improvements thus far, despite using highly efficient SF chromophores.^{4–6} Design of such devices must therefore also consider the processes involved in harvesting triplet excitons produced by SF. The migration of these excitons to interfaces or junctions at which either energy or charge transfer can occur plays a significant role, and hence must be well understood in order to design PV devices in which SF yields an appreciable efficiency increase.

Triplet exciton transfer is generally understood as a short-range, incoherent process that may be described as ‘hopping’ of excitons between chromophore sites.⁷ As such, triplet mobility is often considered in terms of a diffusive random walk, with an effective diffusion coefficient describing the rate of triplet migration throughout the material.^{8–10} Models used to describe this behavior are generally derived from the seminal work of Smoluchowski, who developed an analytical solution for the three-dimensional coagulation of equivalent particles controlled by diffusive motion.^{11,12} However, such models usually assume an isotropic medium in which these particles (or quasi-particles in the case of excitons) may diffuse, while the library of known SF-capable chromophores primarily consists of π -conjugated organic molecules with significant structural anisotropy in two or three dimensions.¹³ Substantial anisotropy may therefore exist in triplet exciton diffusion rates along different crystallographic axes of organic SF chromophores. As a case in point, preferential triplet migration along a single axis was observed by transient absorption microscopy in a series of SF-capable acenes.¹⁴ More recently, the rates of diffusion-controlled triplet–triplet annihilation (TTA) along different crystallographic axes in hexacene were shown to vary by a factor of four, attributed to different modes of crystal packing along these axes.¹⁵ It is hence becoming clear

that such anisotropic diffusion plays a significant role in triplet exciton migration through crystalline organic systems, and must be accounted for when designing PV devices containing these materials as SF chromophores.

6,13-(triisopropylsilylethynyl)pentacene (TIPS-Pn) is an intensely studied model SF chromophore, in which the SF process is slightly exoergic.¹³ In its crystalline phase, SF has been shown to occur on sub-picosecond timescales^{16,17} and with effectively quantitative yield of triplets.¹⁸ The dominant crystal polymorph of TIPS-Pn consists of an extended slip-stacked structure with significant π - π stacking in two dimensions, but contact only through insulating TIPS groups along the third crystallographic axis.^{19,20} This π -stacking is unequal in both slip-stacked directions; a recent computational study predicted electron and hole transfer integrals to differ by up to a factor of 8 between the different slip-stacked pairs on this plane.¹⁰ Despite this significant structural anisotropy between all three crystallographic axes, previous studies of triplet diffusion in crystalline TIPS-Pn have assumed purely isotropic migration.^{10,21} Such treatments are unlikely to accurately describe triplet exciton diffusion within TIPS-Pn, and may therefore give incorrect or misleading predictions when designing systems that depend upon triplet diffusion through TIPS-Pn. This issue is especially relevant given recent advancements in solution-coating methods, as solution-sheared layers of TIPS-Pn with single-crystal alignment on the order of millimeters have been recently reported.^{20,22,23} On such a large length scale, even small inaccuracies in describing exciton diffusion rates would manifest in substantial errors in predicted exciton diffusion distances along different crystallographic axes. As such, it is necessary to develop further understanding of the anisotropic nature of exciton diffusion in crystalline TIPS-Pn.

In this work, we study triplet diffusion through crystalline nanoparticles (NPs) of TIPS-Pn using femtosecond transient absorption (TA) spectroscopy. The decay kinetics of triplet excitons arising from SF are shown to depend strongly on excitation density, indicative of bimolecular exciton-exciton annihilation. These kinetics are well fit by a model that assumes isotropic three-dimensional triplet exciton diffusion, but yield best-fit parameters that are

physically unreasonable when considering the intermolecular packing of crystalline TIPS-Pn. However, this annihilation is also well-modeled by considering diffusion mostly along a single axis and yields physically reasonable fit parameters, suggesting that diffusion through TIPS-Pn is highly anisotropic on the timescale considered here. This result agrees with diffusion coefficients predicted by density functional theory (DFT), which indicate that diffusion along the a -axis of crystalline TIPS-Pn is faster than diffusion through next-nearest-neighbor stacking within the crystal by a factor of 25. This anisotropy highlights the importance of controlling chromophore morphology in the fabrication of SF-sensitized organic PV devices, as it may enable rapid and directional triplet exciton transport in single-crystal TIPS-Pn films.

Methods

Materials

TIPS-Pn was used as-purchased from Ossila. Poly(vinyl alcohol) (PVA; Merck, average molecular weight 130 kg/mol) was sourced as a solid powder, and dissolved to a stock concentration of 10 mg/mL by heating at 90 °C in water for 1 hour. Water was purified by an 18 M Ω Millipore Milli-Q Reagent Water System fitted with a 0.45- μ m filter. HPLC-grade tetrahydrofuran (THF; RCI Labscan) was freshly distilled before use.

Nanoparticle Preparation

Crystalline TIPS-Pn nanoparticles were prepared using a previously described procedure.¹⁷ Briefly, TIPS-Pn in THF (200 μ L, 800 μ M) was flash-precipitated into rapidly-stirred water (10 mL), yielding an aqueous suspension of amorphous-phase TIPS-Pn nanoparticles. This process was repeated twice, and the resulting suspensions combined and concentrated under reduced pressure to a final TIPS-Pn concentration of 100 ppm. The suspension of nanoparticles was filtered through a 0.2- μ m syringe filter (Sartorius Minisart NML). A 20 μ L portion of PVA solution (10 mg/mL) was then added to 1.98 mL of NP suspension, and the nanoparticles allowed to crystallize for 16 hours. Dynamic light scattering (DLS) characterization of nanoparticle size was conducted with a Malvern Zetasizer Nano ZSP, using a 633-nm laser at a backscattering angle of 173°.

Spectroscopic Measurements

All spectroscopic measurements were collected in a 2-mm path length quartz cuvette (Starna Cells 21-Q-2). Steady-state absorption spectra were collected using a Cary Varian 1E UV-visible spectrophotometer. Time-resolved spectroscopic measurements were collected on a transient absorption spectrometer (Ultrafast Systems, Helios). Laser pulses at 800 nm with a 100-fs pulse width and 1-kHz repetition rate were generated as the primary light source

using a Ti:sapphire regenerative amplifier (Spectra Physics, Spitfire Pro XP 100F). An optical parametric amplifier (Light Conversion, TOPAS-C) was used to produce 440-nm pump pulses from the fourth harmonic of the idler, with a spot-size of 465 μm at the sample position. Pump fluences were varied from 20 $\mu\text{J cm}^{-2}$ to approximately 1 mJ cm^{-2} . Focusing of the 800-nm pulses onto a 3.2-mm sapphire crystal generated white-light continuum probe pulses with a spectral coverage of 450–750 nm and a spot-size of 122 μm at the sample position. Pump and probe were polarized at the magic angle of 54.7° relative to one another in order to minimize polarization biases in the measurements. Nanoparticle suspensions were constantly stirred during experiments, with negligible photo-bleaching observed.

Computational Details

Density functional theory (DFT) calculations were performed using the Q-Chem computational chemistry software package, version 5.2.2.²⁴ All calculations were run at the PBE/6-31G* level of theory,^{25,26} as it has been previously used to give reasonable predictions of triplet diffusion rates in other polyaromatic hydrocarbons.⁷ Electronic couplings were computed by constrained DFT configuration-interaction (CDFT-CI) calculations of TIPS-Pn dimer pairs taken from the crystal structure reported by Anthony and co-workers.^{19,27} Given that the solubilizing silyl groups in TIPS-Pn have a minimal influence on triplet energetics, isopropylsilyl groups were replaced by methyl groups in these calculations to reduce computational expense. In each state, one monomer was constrained to triplet spin and the other to singlet spin. Further details of these calculations are given in Section S9 of the Supporting Information (SI).

Results and Discussion

Size characterization by DLS (SI, Section S1) shows that a monodisperse size distribution of nanoparticles (z-average diameter of 72 nm) results from the preparation method employed here. This is in close agreement with other size distributions previously reported for TIPS-Pn NPs prepared through this method.^{17,18} Additionally, steady-state absorption (SI, Section S3) and femtosecond TA spectra (Figure 1) of these NPs are identical to those reported in our previous study of crystalline TIPS-Pn NPs, in which X-ray diffraction was used to confirm that the chromophores adopted the slip-stacked morphology characteristic of crystalline TIPS-Pn.¹⁷ Therefore, we conclude that the TIPS-Pn NPs studied here possess a crystalline morphology with the slip-stacked packing motif first reported by Anthony and co-workers.¹⁹

Figure 1a shows representative TA spectra of crystalline TIPS-Pn NPs at delay times ranging from 200 fs to 3 ns. Excited-state absorption (ESA) features at 488, 523 and 750 nm are observed to rise within 1 ps, concomitant with the decay of other ESA bands at 460 and 620 nm. These bands have been previously assigned to the triplet state (T_1) and singlet state (S_1) of TIPS-Pn, respectively.^{16,21} This rapid interconversion is indicative of singlet fission occurring on a sub-picosecond timescale in crystalline TIPS-Pn, agreeing with multiple previous studies.^{10,17,28} Subtle restructuring of the triplet ESA bands at 488 and 523 nm then occurs over several picoseconds, with these features slightly red-shifting and the longer-wavelength band becoming more intense. This has previously been attributed to spatial separation of the correlated triplet pair state, and so we assign this spectral change to the formation of free triplet excitons from correlated triplet pairs.¹⁸ The transient spectra then decay, with negligible further spectral evolution beyond 50 ps (Figure 1b), indicating minimal further relaxation within the triplet excited-state manifold, with these triplet states only decaying to the ground state. Therefore, we assign these TA spectra from 50 ps onwards as being predominantly due to free triplet excitons within crystalline TIPS-Pn, with negligible contributions from singlet excitons and no further separation of any correlated triplet pair

excitons.

The ESA at 680 nm and the ground-state bleach (GSB) at 700 nm red-shift slightly at delay times beyond 50 ps, which becomes increasingly evident at high pump fluences (SI, Section S2). This spectral shift may be due to a change in the nature of the GSB itself. A recent study by Jones and co-workers identified a lower energy shoulder in the main absorption band of crystalline TIPS-Pn, which they assigned to excitations of non-equilibrium crystal packings induced by grain boundaries or defect sites.²⁹ Should such lower energy sites exist in the nanoparticles studied here, they may act as trap sites, with triplet excitons funneled to these sites due to the surrounding energy gradient. This process would result in a shift in the relative exciton populations at equilibrium and non-equilibrium TIPS-Pn sites over time, yielding a corresponding shift in the GSB due to the spectral differences of these sites in their ground states.

The decay of the 523 nm ESA signal depends strongly upon pump fluence: as demonstrated in Figure 1c, this decay accelerates at higher pump fluences. This behavior is indicative of bimolecular exciton–exciton annihilation interactions dominating the triplet decay at the excitation densities used here.^{10,18,21} To quantify these annihilation interactions, we consider a number of bimolecular annihilation kinetic models to fit to the data collected here. All models considered have the general form

$$\frac{d[T]}{dt} = -k_1[T] - k_2[T]^2, \quad (1)$$

where k_1 is the unimolecular rate coefficient associated with first-order triplet decay and k_2 is the bimolecular annihilation rate coefficient. Assuming isotropic diffusion of triplet excitons and that annihilation is effectively instantaneous upon contact, k_2 may be related to the diffusion constant D and annihilation radius R of triplet excitons by^{11,12}

$$k_2 = 8\pi RD \left(1 + \frac{R}{\sqrt{2\pi Dt}} \right). \quad (2)$$

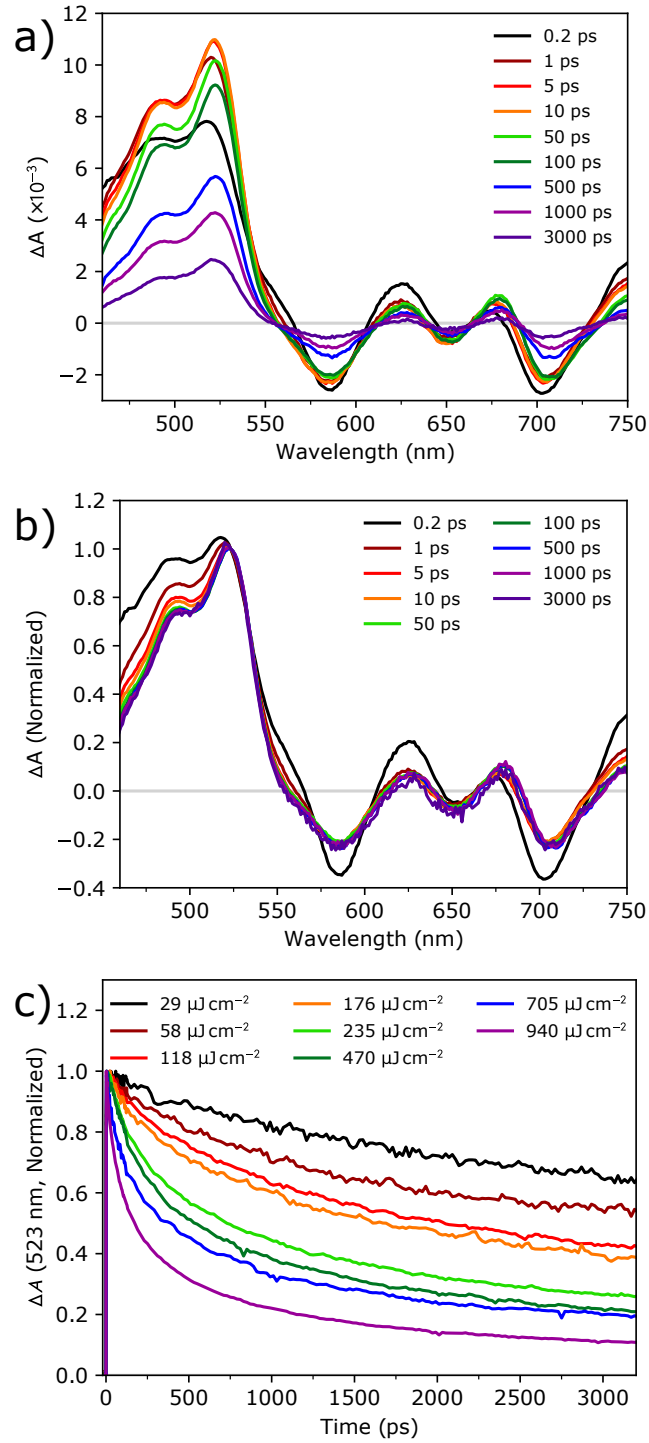


Figure 1: TA spectra of crystalline TIPS-Pn NPs after excitation at 440 nm at a pump fluence of $470 \mu\text{J cm}^{-2}$, as (a) measured ΔA and (b) ΔA normalized to the 523 nm triplet ESA feature. (c) Normalized decay kinetics of the 523 nm triplet ESA under a range of pump fluences.

At long times for which $\sqrt{2\pi Dt} \gg R$, eq 2 reduces to

$$k_2 = 8\pi RD. \quad (3)$$

The approximation in eq 3 has been widely used to describe bimolecular annihilation for excitons encountering one another through a three-dimensional random walk.^{30,31} Several previous studies have applied eq 3 to model the bimolecular annihilation kinetics of pentacene⁹ and TIPS-Pn.^{10,21} While both equations stem from the same model, they are qualitatively different: one treats the exciton annihilation rate coefficient as time-independent, while the other also includes a time-dependent component on short timescales. We consider both forms of this model when attempting to fit the TA data here, and refer to them below as the “constant k_2 ” and “time-dependent k_2 ” isotropic 3D diffusion models, respectively.

Triplet concentrations within the nanoparticles were extracted from the TA data (see SI Section S3 for details), and both isotropic 3D models presented above were fit to the data over a range of excitation densities. Figure 2 shows a sample of the fits at pump fluence of 470 pJ cm^{-2} , while the remaining fits are shown in the SI (Section S4). When considering the isotropic 3D diffusion models, the time-dependent k_2 model (solid curve, coincident with the dashed curve) fits the data significantly better than the constant k_2 model (dotted curve), with the latter underestimating the decay rate at early times and overestimating at later times. Clearly, the time-dependent nature of the triplet annihilation rate coefficient due to diffusion must be accounted for on the sub-nanosecond timescale when describing excitonic migration within crystalline TIPS-Pn. As such, the isotropic 3D diffusion model with constant k_2 is excluded from the following discussion, and the time-dependent k_2 model is hereafter referred to as the “isotropic 3D diffusion model” for simplicity.

The best-fit parameter values for the isotropic 3D diffusion model are shown in Table 1. Using the best-fit R and D values in the long-time limiting case (eq 3), a bimolecular annihilation constant of $(1.2 \pm 0.2) \times 10^{10} \text{ M}^{-1} \text{ s}^{-1}$ is obtained, which agrees closely with a previous

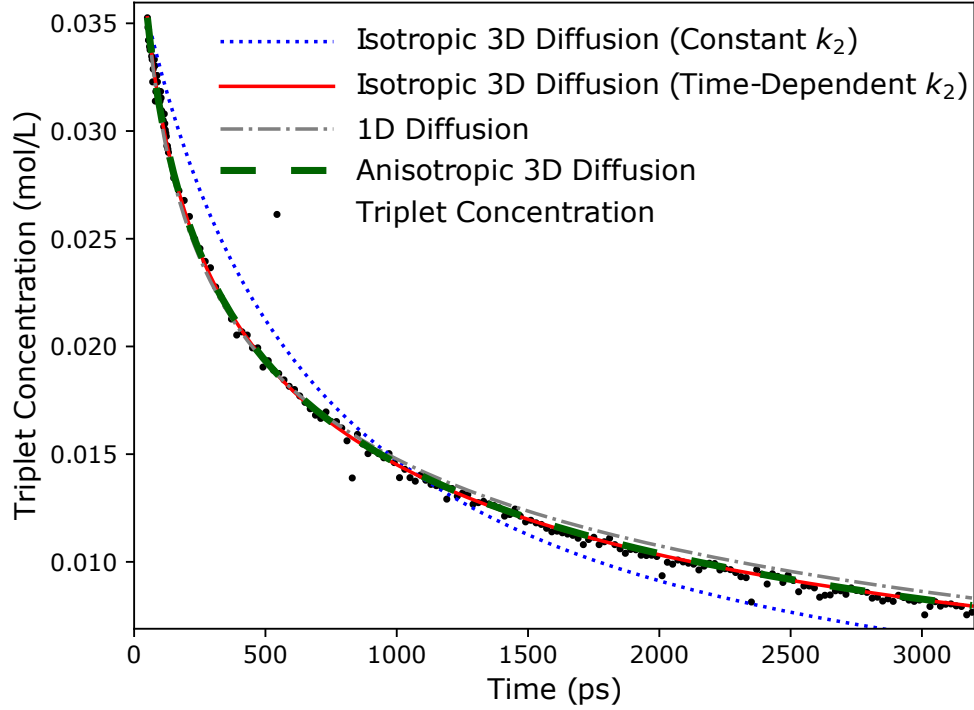


Figure 2: Triplet concentrations in crystalline TIPS-Pn NPs from 50 ps after excitation with pump fluence of $470 \mu\text{J cm}^{-2}$, with fits from all bimolecular annihilation models considered here. Best-fit parameters from models of interest are shown in Table 1. Note that the fits from the isotropic 3D (time-dependent k_2) and anisotropic 3D models are coincident.

measurement for polycrystalline TIPS-Pn thin-films.²¹ Additionally, with these values of R and D , eq 3 is expected to be valid on timescales much longer than 10^{-9} s. Therefore, the short-time behavior of eq 2 is irrelevant on timescales longer than nanoseconds. This result may help to reconcile the apparent discrepancy between the fitting of time-dependent spectral data on triplet populations here and in other reports; previous studies of TTA in TIPS-Pn have generally focused upon timescales of 10^{-8} – 10^{-6} s,^{10,14,21} in which eq 3 is a good approximation of eq 2. This study, however, considers diffusion on a significantly shorter timescale, for which the time-dependent form of k_2 is necessary to adequately describe bimolecular TTA in TIPS-Pn.

The first-order rate constants (k_1) obtained from all diffusion models considered here (Table 1) correspond to intrinsic triplet lifetimes on the order of tens to hundreds of nanoseconds, which are significantly shorter than the timescale of microseconds previously reported for TIPS-Pn.^{14,21} While accurate fitting of such a slow process from the 3-ns time window observed here is not expected, these rapid decays are unusual. This first-order term is necessary to adequately fit the data, as using only the bimolecular term is insufficient to capture all of the triplet decay (SI, Section S5). Several other studies using ps–ns TA have also reported first-order triplet decays on similar timescales for TIPS-Pn.^{32–34} One possible explanation for this behavior is geminate TTA. While the triplet ESA signals observed here show negligible spectral evolution beyond 50 ps after excitation, it is possible that some triplet pair states may still be present, as correlated triplet pairs and free triplets in crystalline TIPS-Pn are spectrally similar in the visible region.^{18,34} It has recently been demonstrated that the singlet fission kinetics in amorphous TIPS-Pn could only be fully described when including a population of triplet pair states that underwent fast non-radiative decay.^{32,35} It was suggested that this may be due to certain TIPS-Pn pair geometries being unsuitable for triplet pair separation, with diffusion away from these sites inhibited. We hypothesize that a similar phenomenon may occur in the crystalline TIPS-Pn NPs studied here, with a relatively small population of triplet pair states unable to separate into free triplets. These triplet

pairs would therefore be unable to undergo bimolecular annihilation in the crystal bulk, and would instead recombine with first-order kinetics.

An alternative cause of this rapid first-order decay in triplet concentration could be triplet-charge annihilation (TCA). We have previously demonstrated that TIPS-Pn NPs re-precipitated into water acquire a negative surface charge, which improves the colloidal stability of these suspensions.¹⁷ Encounters between these charges and triplet excitons could result in exciton annihilation that is pseudo first-order with respect to triplet concentration, as has previously been reported in other organic semiconductors.^{36,37} By considering the rate at which triplets diffuse to charged sites at the NP surface, whose density was estimated from experimental zeta potential measurements, we estimate that TCA in the TIPS-Pn NPs studied here could occur on a time scale of 10^{-8} – 10^{-5} s, based on the diffusion coefficients in Table 1 and the conservative assumption that every triplet-charge encounter leads to exciton annihilation (SI, Section S6). These values are consistent with the best-fit first-order decay coefficients from the experimental data. However, there is a significant level of uncertainty in these estimates, which precludes us from assigning the extent to which TCA contributes to this first-order decay. Scattering of the laser pulse was also considered as an alternative process that could result in this rapid first-order triplet decay (SI, Section S6), but was discounted as a major contributor as it could only occur on a time scale much slower than the first-order rate coefficients fit here.

Table 1: Best-Fit Parameters for 1D and 3D Diffusion Models Fit to Triplet Exciton Concentrations in Crystalline TIPS-Pn NPs^a

Diffusion Model	D (cm ² s ⁻¹)	R (nm)	k_1 (10 ⁷ s ⁻¹)	χ^2 (10 ⁻⁴ M ²) ^b
Isotropic 3D	$(3.5 \pm 0.5) \times 10^{-6}$	2.3 ± 0.1	0.6 ± 0.5	1.87
1D	$(3.52 \pm 0.06) \times 10^{-3}$ ^c	0.7565^c	7.9 ± 0.4	2.52
Anisotropic 3D	$(2.5 \pm 0.1) \times 10^{-3}$ ^{c,d}	0.7565^c	2.3 ± 0.6	1.88

^a Uncertainties are 95 % confidence intervals estimated from the fitting process.

^b χ^2 denotes the sum of squared residuals between the model and experimental triplet concentrations.

^c Assumes R_{1D} to be equal to the a -axis lattice spacing of 7.565 Å.

^d Diffusion coefficient along the fast axis (D_z); a separate coefficient of $D_\rho = (1.1 \pm 0.3) \times 10^{-7}$ cm² s⁻¹ is fit in the slower direction.

The best-fit value of D determined from the isotropic 3D model is of a similar order of magnitude to that previously determined for polycrystalline TIPS-Pn.^{10,21} However, the annihilation radius R is much larger than what has been previously considered physically reasonable for TIPS-Pn. Triplet excitons are generally understood to be highly localized upon single chromophores, with hopping limited to nearest-neighbors by Dexter-type energy transfer.^{7,38} Given the close intermolecular contacts within slip-stacked TIPS-Pn, an annihilation radius on the order of 1 nm or less has been previously predicted for triplet excitons in TIPS-Pn.^{14,21} However, these previous studies were unable to independently determine both R and D as they used eq 3 to model the long-time triplet diffusion in crystalline TIPS-Pn. In contrast, the fitting of eq 2 to early-time data here allows for independent extraction of these two parameters, but yields a best-fit value of R as 2.3 nm, which is clearly incongruent with these previous estimates. We considered the possibility that this large value may have arisen due to poor sensitivity of the fitting process to variations in the value of R , and attempted to fit this model with R constrained to more physically reasonable values. However, reduction of R below 1.8 nm reduced the quality of the fit to the experimental data and yielded unreasonably low values of the rate coefficient k_1 for first-order triplet decay (SI, Section S7). Therefore, we discount this factor as a source of error for the large value of R determined here.

However, both of the diffusion models considered so far assume that triplet excitons diffuse isotropically in three dimensions through TIPS-Pn, which is highly unlikely given the significant anisotropy within the crystal packing. As shown in Figure 3a, preferential exciton migration through the ab plane of the material would be expected, as the slip-stacked morphology provides π -stacking interactions and hence relatively large electronic couplings between chromophores in these directions.¹⁹ Conversely, hopping in the c -direction should be significantly slower, as the TIPS-Pn molecules contact one another only through insulating TIPS-groups in this direction (Figure 3b). The good fit of the isotropic 3D diffusion model to the experimental data in Figure 2 despite the 3D anisotropy of TIPS-Pn can be rationalized

as follows. The rate coefficients for bimolecular reactions limited by anisotropic 3D diffusion have been shown for various cases of anisotropy in either the diffusion tensor or reaction volume to obey an equation of the general form^{39,40}

$$k_2 = B + \frac{C}{\sqrt{t}}, \quad (4)$$

for some constants B and C . However, the relationship between these constants and physical parameters depends on the anisotropy of the diffusion tensor or reaction (annihilation) volume. As eq 2 for isotropic 3D diffusion is equivalent in form to eq 4, the isotropic 3D diffusion model may therefore fit the data well even if diffusion is highly anisotropic in the measured system, but with best-fit parameters that may not be physically meaningful. This consideration may hence explain the unreasonably large best-fit value of R determined from the fitting here. We therefore offer a cautionary note: while 3D isotropic diffusion models similar to those used here are commonly used to explain exciton migration in organic materials,^{8–10,21,32} the diffusion coefficients and annihilation radii resulting from this fitting may not correspond to the material’s true, physical properties, and should be interpreted with care.

Given the significant anisotropic packing of crystalline TIPS-Pn, it is reasonable to question whether a full 3D treatment of diffusion is necessary to describe bimolecular TTA. Due to the exponential decrease of the Dexter energy transfer rate constant with interchromophore distance,⁴¹ long-distance hopping along the c -axis should contribute negligibly to overall exciton diffusion. Additionally, π - π stacking is most significant along the a -axis, so triplet energy transfer is expected to be fastest along this axis. This directional triplet transfer is supported by a previous transient absorption microscopy study of triplet migration in single-crystal TIPS-Pn, which found that triplet diffusion was anisotropic on the ab -plane and fastest along the a -axis.¹⁴ Therefore, we hypothesized that triplet diffusion in TIPS-Pn on the sub-nanosecond timescale could be approximated by one dimensional (1D) diffusion

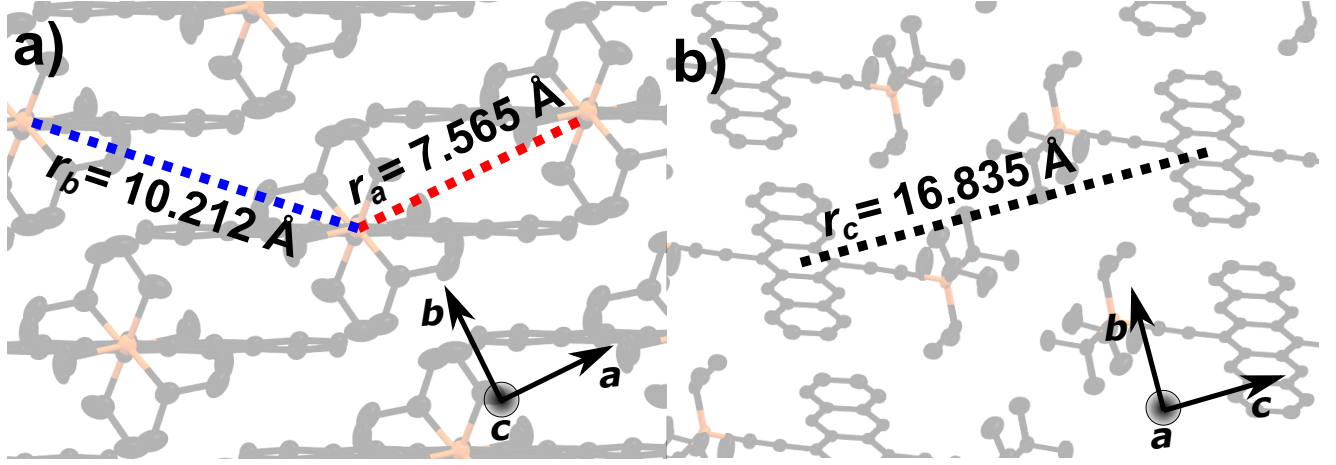


Figure 3: Crystal packing of the primary polymorph of crystalline TIPS-Pn in the (a) ab -plane and (b) bc -plane. Dashed lines represent intermolecular packing distances, with unit cell axes shown from each perspective for reference. Carbon atoms are shown in black and silicon atoms in orange; hydrogen atoms are omitted for clarity. The crystal structure is taken from ref. 19.

along the a -axis. To test this hypothesis, we considered a model in which diffusion is only allowed in a single dimension,⁴²

$$k_2 = \frac{1}{R_{1D}N_0} \sqrt{\frac{8D_{1D}}{\pi t}}, \quad (5)$$

where N_0 is the average molecular density throughout the system (calculated from the density and molecular weight of TIPS-Pn; SI, Section S8), and R_{1D} and D_{1D} are 1D analogues of the parameters discussed above. When applying this model to the experimental data here (Figure 2, dot-dashed curve and SI, Section S4), a relatively good fit to the data is observed. The 1D model captures much of the triplet decay kinetics, and fits the data almost as well as the isotropic 3D diffusion model at early times (< 1 ns). Therefore, the TTA kinetics studied here may be reasonably approximated by diffusive motion in only a single dimension on the sub-nanosecond timescale. Like eq 2 for isotropic 3D diffusion, eq 5 for 1D diffusion is equivalent in form to eq 4, but has a different relationship between the constants B and C and physical parameters (notably $B = 0$ for 1D diffusion). Therefore, this fit yields very different values for these parameters compared with the analogous parameters in the

isotropic 3D model. Due to the nature of eq 5, R_{1D} and D_{1D} are not separable when fitting this model, but the term $D_{1D}^{1/2} R_{1D}^{-1}$ fits as a single parameter. However, if it is assumed that R_{1D} corresponds to the nearest-neighbor stacking distance along the a -axis of 7.565 Å, fitting this model to the data yields a 1D diffusion coefficient of $3.52 \times 10^{-3} \text{cm}^2 \text{s}^{-1}$, which agrees closely with the 1D diffusion coefficient determined by Zhu and co-workers' study of single-crystal TIPS-Pn.¹⁴ This relatively good fit to the data and agreement with another study suggests that exciton diffusion along the a -axis dominates the bimolecular TTA in crystalline TIPS-Pn on the sub-nanosecond timescale.

However, the 1D diffusion model does not fit the experimental data as well the isotropic 3D model over the entire time window observed here; at later times ($> 1 \text{ ns}$) it begins to underestimate the rate of triplet decay. This discrepancy suggests that slow but non-negligible diffusion may occur along other crystallographic axes of TIPS-Pn, which is not included in the 1D model. To account for this, we considered an expanded model in which diffusion is still fastest along a single axis, but a slower rate of diffusion in the directions perpendicular to this are still permitted. For simplicity, this model assumes that the rates of diffusion along both axes perpendicular to the direction of fast diffusion are equivalent. In this “anisotropic 3D diffusion model”, the bimolecular rate constant is given by³⁹

$$k_2 = 16 \sqrt{\frac{D_z D_\rho}{\pi R_z N_0}} + \frac{1}{R_z N_0} \sqrt{\frac{8 D_z}{\pi t}}, \quad (6)$$

where D_z and D_ρ represent the diffusion coefficients in the fast and slow directions, respectively, and R_z is the annihilation radius along the direction of fast motion (the correspondence to equations in ref 37 is obtained by noting that $(R_z N_0)^{-1} = \pi R_\rho^2$, where R_ρ is the average annihilation radius in the directions perpendicular to the fast direction, assuming annihilation between excitons on nearest-neighbor molecules). Again, this model has the same general form as eq 4, and as D_ρ approaches zero eq 6 reduces to the 1D diffusion model. Fits of the anisotropic 3D diffusion model to the experimental data are shown in Figure 2

(dashed curve) and Section S4 of the SI, with best-fit parameters in Table 1. As with the 1D model, the annihilation radius R_z is constrained to the a -axis molecular displacement during the fitting process. The anisotropic 3D diffusion model shows an improved fit over the 1D model, fitting the experimental data equally as well as the isotropic 3D diffusion model. The similarity in the fits of the isotropic and anisotropic 3D diffusion models to the data is again due to the equivalence of their functional forms (eq 4), but these models have significantly differing relationships between coefficients B and C and physical parameters. This result again highlights the issue identified above with using isotropic diffusion models to describe anisotropic diffusion: the model may fit the data well, but the best-fit parameters may not have the expected relationship to the material’s physical properties.

The two diffusion coefficients fit to the anisotropic 3D diffusion model differ by four orders of magnitude. The fast diffusion coefficient D_z is comparable to D_{1D} fit from the 1D diffusion model, while D_ρ is four orders of magnitude smaller. This result supports the earlier hypothesis that triplet exciton diffusion in crystalline TIPS-Pn is fastest along the a -axis, with significantly slower diffusion occurring in the directions perpendicular to this. However, the anisotropic 3D diffusion model assumes that diffusion both of these perpendicular directions are equivalent, which is likely not the case in crystalline TIPS-Pn. As demonstrated in Figure 3, molecular packing modes along the b - and c -axes are substantially different from one another, and so the rates of diffusion in each of these directions are likely also inequivalent. D_ρ should therefore be considered some form of averaged diffusion coefficient along these two axes, but the exact contributions from each of these directions cannot be determined from this model.

To verify our measurements of anisotropic diffusion in TIPS-Pn, DFT and Marcus theory were used in combination to estimate triplet hopping rates and diffusion coefficients along different packing directions of crystalline TIPS-Pn, as per the method reported by Yost *et al.*⁷ Triplet energy transfer requires an effective transfer of two electrons between donor and acceptor sites, and so is commonly approximated by Marcus electron-transfer theory.⁷ In

Marcus theory, the rate coefficient for electron transfer between a donor site and an acceptor site is given by

$$k_{\text{da}} = \frac{2\pi}{\hbar} |V_{\text{da}}|^2 \sqrt{\frac{1}{4\pi k_{\text{B}} T \lambda}} \exp \left[-\frac{(\Delta G^\circ + \lambda)^2}{4\lambda k_{\text{B}} T} \right], \quad (7)$$

where V_{da} is the electronic coupling between donor and acceptor diabatic states, T is temperature, λ is the reorganization energy, ΔG° is the free energy change upon transfer and k_{B} is the Boltzmann constant.⁴³ ΔG° is zero for triplet excitons hopping through an infinite crystalline lattice, as adjacent lattice sites are equivalent in crystalline TIPS-Pn. λ was calculated at the PBE/6-31G* theory level using the four-point method on a single molecule of TIPS-Pn,^{7,25,26} and V_{da} was determined by CDFT-CI calculations between each unique dimer pair at the same level of theory.²⁷ Further details of these calculations are shown in the SI, Section S9. The hopping rate coefficient can then be related to the one-dimensional diffusion coefficient along each axis by⁴⁴

$$D_{1\text{D}} = \frac{a^2}{2} k_{\text{da}}, \quad (8)$$

where a is the lattice parameter along this axis.

Predicted hopping rate coefficients and diffusion coefficients along the a , b and c stacking directions (denoted as r_a , r_b and r_c , respectively, in Figure 3) are shown in Table 2. While r_a and r_c correspond to the crystallographic a and c axes of crystalline TIPS-Pn, respectively, r_b does not fully align with the b -axis. Therefore, we hereafter refer to the “ b slip-stacking direction” or “ b molecular pair” to avoid confusion with the crystallographic b -axis. Triplet hopping and diffusion is predicted to be faster along the a -axis relative to the b -stacking direction by over an order of magnitude, with diffusion along the c -axis slower again by at least five orders of magnitude. The predicted diffusion coefficient along the a -axis agrees relatively well with the best-fit values of $D_{1\text{D}}$ and D_z from the experimental data (given the low level of computational theory used), differing by only a factor of 2–3. Additionally, the best-fit value of D_ρ from the anisotropic 3D diffusion model is on the same order of

magnitude as the geometric mean of the predicted diffusion coefficients along the b and c packing directions ($6.4 \times 10^{-7} \text{ cm}^2 \text{ s}^{-1}$). These results therefore support the above conclusions from fitting to the experimental data, indicating that triplet exciton diffusion occurs predominantly along the a -axis on short timescales, with significantly slower diffusion in the b -direction and negligible diffusion along the c -axis.

Table 2: Predicted Electronic Couplings, Hopping Coefficients and Diffusion Coefficients for Triplet Excitons Between Different Molecular Pairs within the TIPS-Pn Crystal Structure.

TIPS-Pn Pair	V_{da} (meV)	k_{da} (ps^{-1})	$D_{1\text{D}}$ ($\text{cm}^2 \text{ s}^{-1}$)
a	7.92	3.70×10^{-1}	1.06×10^{-3}
b	1.16	7.94×10^{-3}	4.14×10^{-5}
c	$< 1 \times 10^{-3}$	$< 7 \times 10^{-9}$	$< 1 \times 10^{-10}$

Such anisotropy in the diffusion of triplet excitons through crystalline TIPS-Pn has significant implications when considering the design and fabrication of any device using TIPS-Pn as an excitonic down-converter. The triplet diffusion length through crystalline TIPS-Pn can be determined by

$$L_{\text{D}} = \sqrt{D\tau}, \quad (9)$$

where τ is the intrinsic lifetime of the triplet excitons. Under conditions of solar flux, bimolecular TTA is expected to be negligible (SI, Section S10), so we consider τ to correspond to the previously reported natural triplet lifetime of $2.1 \mu\text{s}$.²¹ Using the 1D diffusion coefficients derived computationally here, eq 9 yields diffusion lengths of 470 nm, 93 nm and < 1 nm along the a -axis, b -stacking direction and c -axis of TIPS-Pn, respectively. That is, triplet excitons in crystalline TIPS-Pn may diffuse over $5\times$ further along the a -axis than the b -stacking direction throughout the exciton lifetime. The predicted diffusion length along the c -axis is smaller than the intermolecular separation in this direction, highlighting that diffusion in the c -direction of crystalline TIPS-Pn is negligible within the triplet lifetime.

The predicted triplet diffusion lengths for the a and b stacking directions are both exceptionally large given the poor mobilities of triplet excitons in organic materials.^{7,45} However,

these values assume diffusion through single-crystal TIPS-Pn, with no polycrystallinity or grain boundaries between crystalline domains. As demonstrated by the significant disparity between hopping rate coefficients along different directions in Table 2, any disruption of the TIPS-Pn slip-stacking will substantially slow triplet mobility through the material. We therefore suggest that the triplet diffusion length in crystalline TIPS-Pn is largely limited by grain boundaries between crystalline domains, and that triplet excitons will accumulate at such boundaries over time. This suggestion agrees with the assignment of the spectral red shifts observed here (SI, Section S1) as an accumulation of excitons at low-energy defect sites such as those at grain boundaries. A significant proportion of TIPS-Pn thin-film systems reported in the literature are polycrystalline in nature,^{10,21,34,46–54} and may therefore experience this phenomenon. Additionally, even for films that achieve large-scale crystalline alignment, the relative orientation of these slip-stacking directions to the device architecture must also be considered. To achieve optimal exciton transfer to an electron accepting layer, the film should be oriented with the a -axis perpendicular to the interface with this layer. Recently, multiple reports have emerged of solution-sheared layers of TIPS-Pn that have large-scale single-crystal alignment with the a -axis oriented perpendicular to the substrate surface.^{20,22,23} Such alignment would allow for fast, directional diffusion of triplet excitons to interfaces with acceptor materials at early times, and would therefore be optimal for SF down-conversion layers in PV devices.

Finally, we note that our analysis until this point has neglected the spin statistics of TTA in TIPS-Pn. For two encountering triplet excitons, a manifold of nine encounter states are possible; one singlet, three triplets and five quintets (assuming degeneracy of encounter states).³⁰ Previous treatments of TTA in organic crystals have attempted to account for this by including a pre-factor of $1/9$ in eq 2, as only one out of the possible nine resulting encounter states results in the removal of two triplet excitons.⁵⁵ In practice, contributions from quintet encounter states are generally neglected, as they are usually so high in energy that they are effectively inaccessible,⁵⁶ thus revising this factor to $1/4$ (three triplet states and

one singlet state). However, recent studies have shown quantum yields of fluorescence from TTA in rubrene and anthracene surpassing this limit.^{57,58} These findings were ascribed to the energy of the T_2 state in these systems being significantly higher than twice the T_1 energy and thus minimizing annihilation occurring through the triplet manifold, as annihilation through the triplet channel requires the formation of one high-energy triplet state from two lower-energy triplets. Indeed, upon observing similar results, Auckett and co-workers suggested that no such spin-statistical limit exists for TTA in rubrene.⁵⁹ To assess whether such a spin-statistical limit of TTA should be considered here, we examined the energies of the low-lying singlet and triplet excitons in crystalline TIPS-Pn (energy level diagram shown in SI Section S11). While the S_1 state of crystalline TIPS-Pn is approximately isoergic with twice the energy of the T_1 state, the T_2 energy is almost 0.4 eV higher in energy than S_1 . This energy difference is greater than $k_B T$ by over an order of magnitude at room temperature, indicating that high-lying triplet states should be effectively inaccessible from TTA under ambient conditions. Therefore, crystalline TIPS-Pn is likely to behave similarly to anthracene and rubrene, with singlet encounter states contributing more to TTA than the prediction from the spin-statistical limit. Annihilation via triplet encounter states may still occur, however the relative contributions of singlet and triplet encounter states cannot be accurately predicted for TIPS-Pn purely from the statistics of encounter state spins. Therefore, the best-fit parameters presented in Table 1 represent the limiting case in which all triplet-triplet encounters result in mutual annihilation of both excitons.

Conclusions

In summary, by studying TTA in crystalline TIPS-Pn using femtosecond transient absorption spectroscopy, we have demonstrated that the mobility of triplet excitons is well-described by diffusion that is spatially anisotropic. While the results show a good fit to an isotropic, three dimensional Smoluchowski-type diffusion model, the resulting fit parameters are not physically representative of crystalline TIPS-Pn, due to the inherent anisotropy of this structure and the similar functional form of the time dependence of isotropic and anisotropic diffusion. The results are also well described by a one dimensional diffusion model, indicating that early-time bimolecular TTA in crystalline TIPS-Pn is dominated by exciton diffusion along a single axis. Fits to an anisotropic 3D diffusion model and computationally predicted diffusion coefficients support this finding, suggesting that diffusion along the crystallographic a -axis is at least one order of magnitude faster than any other direction in crystalline TIPS-Pn. Diffusion lengths of 470 nm and 93 nm are predicted for triplet excitons diffusing along the a and b packing directions, respectively, in single crystal TIPS-Pn. This work therefore demonstrates that triplet diffusion along is highly anisotropic in crystalline TIPS-Pn, highlighting the importance of single crystal alignment in promoting efficient exciton transport through TIPS-Pn films.

Supporting Information Description

(1) Characterization of nanoparticle size by dynamic light scattering (2) normalized transient absorption spectra; (3) determination of triplet concentrations from transient absorption data; (4) fit of diffusion models to transient absorption data; (5) fit of the isotropic three-dimensional diffusion model without a first-order decay term; (6) other possible first-order decay processes; (7) fit of the isotropic three-dimensional diffusion model with constrained annihilation radius; (8) calculation of the TIPS-Pn average molecular density; (9) prediction of triplet hopping rates in crystalline TIPS-Pn; (10) annihilation kinetics under solar irradiation; and (11) TIPS-Pn excited-state energies.

Acknowledgments

This work was supported by an Australian Government Research Training Program (RTP) scholarship and funding from the Australian Research Council (DP190102100, DP160103797 and LE0989747). The authors also thank Dr. Patrick Tapping, Alexandra Stuart and Jessica de la Perrelle for stimulating conversations that contributed to this work.

References

- (1) Felter, K.; Grozema, F. C. Singlet Fission in Crystalline Organic Materials: Recent Insights and Future Directions. *J. Phys. Chem. Lett.* **2019**, *10*, 7208–7214.
- (2) Tayebjee, M. J. Y.; Gray-Weale, A. A.; Schmidt, T. W. Thermodynamic Limit of Exciton Fission Solar Cell Efficiency. *J. Phys. Chem. Lett.* **2012**, *3*, 2749–2754.
- (3) Tayebjee, M. J. Y.; McCamey, D. R.; Schmidt, T. W. Beyond Shockley–Queisser: Molecular Approaches to High-Efficiency Photovoltaics. *J. Phys. Chem. Lett.* **2015**, *6*, 2367–2378.
- (4) Jadhav, P. J.; Brown, P. R.; Thompson, N.; Wunsch, B.; Mohanty, A.; Yost, S. R.; Hontz, E.; Van Voorhis, T.; Bawendi, M. G.; Bulović, V. et al. Triplet Exciton Dissociation in Singlet Exciton Fission Photovoltaics. *Adv. Mater.* **2012**, *24*, 6169–6174.
- (5) Lee, J.; Jadhav, P.; Reuswig, P. D.; Yost, S. R.; Thompson, N. J.; Congreve, D. N.; Hontz, E.; Van Voorhis, T.; Baldo, M. A. Singlet Exciton Fission Photovoltaics. *Acc. Chem. Res.* **2013**, *46*, 1300–1311.
- (6) Wilson, M. W. B.; Rao, A.; Ehrler, B.; Friend, R. H. Singlet Exciton Fission in Polycrystalline Pentacene: From Photophysics toward Devices. *Acc. Chem. Res.* **2013**, *46*, 1330–1338.
- (7) Yost, S. R.; Hontz, E.; Yeganeh, S.; Van Voorhis, T. Triplet vs Singlet Energy Transfer in Organic Semiconductors: The Tortoise and the Hare. *J. Phys. Chem. C* **2012**, *116*, 17369–17377.
- (8) Borowicz, B.; Nickel, B. Application of High-Accuracy Time-Resolved Laser Spectroscopy to the Study of Diffusion-Controlled Triplet-Triplet Annihilation. *Opto-Electron. Rev.* **2004**, *12*, 325–332.

- (9) Poletayev, A. D.; Clark, J.; Wilson, M. W. B.; Rao, A.; Makino, Y.; Hotta, S.; Friend, R. H. Triplet Dynamics in Pentacene Crystals: Applications to Fission-Sensitized Photovoltaics. *Adv. Mater.* **2014**, *26*, 919–924.
- (10) Grieco, C.; Doucette, G. S.; Munro, J. M.; Kennehan, E. R.; Lee, Y.; Rimshaw, A.; Payne, M. M.; Wonderling, N.; Anthony, J. E.; Dabo, I. et al. Triplet Transfer Mediates Triplet Pair Separation during Singlet Fission in 6,13-Bis(triisopropylsilylethynyl)-Pentacene. *Adv. Funct. Mater.* **2017**, *27*, 1703929.
- (11) von Smoluchowski, M. Drei Vorträge über Diffusion, Brownsche Bewegung und Koagulation von Kolloidteilchen. *Z. Phys.* **1916**, *17*, 557–585.
- (12) Chandrasekhar, S. Stochastic Problems in Physics and Astronomy. *Rev. Mod. Phys.* **1943**, *15*, 1–89.
- (13) Smith, M. B.; Michl, J. Recent Advances in Singlet Fission. *Annu. Rev. Phys. Chem.* **2013**, *64*, 361–386.
- (14) Zhu, T.; Wan, Y.; Guo, Z.; Johnson, J.; Huang, L. Two Birds with One Stone: Tailoring Singlet Fission for Both Triplet Yield and Exciton Diffusion Length. *Adv. Mater.* **2016**, *28*, 7539–7547.
- (15) Han, J.; Xie, Q.; Luo, J.; Deng, G.-H.; Qian, Y.; Sun, D.; Harutyunyan, A. R.; Chen, G.; Rao, Y. Anisotropic Geminant and Non-Geminant Recombination of Triplet Excitons in Singlet Fission of Single Crystalline Hexacene. *J. Phys. Chem. Lett.* **2020**, *11*, 1261–1267.
- (16) Bakulin, A. A.; Morgan, S. E.; Kehoe, T. B.; Wilson, M. W. B.; Chin, A. W.; Zigmantas, D.; Egorova, D.; Rao, A. Real-Time Observation of Multiexcitonic States in Ultrafast Singlet Fission Using Coherent 2D Electronic Spectroscopy. *Nat. Chem.* **2016**, *8*, 16–23.

- (17) Hudson, R. J.; de la Perrelle, J. M.; Pensack, R. D.; Kudisch, B.; Scholes, G. D.; Huang, D. M.; Kee, T. W. Organizing Crystalline Functionalized Pentacene Using Periodicity of Poly(Vinyl Alcohol). *J. Phys. Chem. Lett.* **2020**, 516–523.
- (18) Pensack, R. D.; Grieco, C.; Purdum, G. E.; Mazza, S. M.; Tilley, A. J.; Ostroumov, E. E.; Seferos, D. S.; Loo, Y.-L.; Asbury, J. B.; Anthony, J. E. et al. Solution-Processable, Crystalline Material for Quantitative Singlet Fission. *Mater. Horiz.* **2017**, *4*, 915–923.
- (19) Anthony, J. E.; Brooks, J. S.; Eaton, D. L.; Parkin, S. R. Functionalized Pentacene: Improved Electronic Properties from Control of Solid-State Order. *J. Am. Chem. Soc.* **2001**, *123*, 9482–9483.
- (20) Diao, Y.; Lenn, K. M.; Lee, W.-Y.; Blood-Forsythe, M. A.; Xu, J.; Mao, Y.; Kim, Y.; Reinspach, J. A.; Park, S.; Aspuru-Guzik, A. et al. Understanding Polymorphism in Organic Semiconductor Thin Films through Nanoconfinement. *J. Am. Chem. Soc.* **2014**, *136*, 17046–17057.
- (21) Grieco, C.; Doucette, G. S.; Pensack, R. D.; Payne, M. M.; Rimshaw, A.; Scholes, G. D.; Anthony, J. E.; Asbury, J. B. Dynamic Exchange During Triplet Transport in Nanocrystalline TIPS-Pentacene Films. *J. Am. Chem. Soc.* **2016**, *138*, 16069–16080.
- (22) Diao, Y.; Tee, B. C. K.; Giri, G.; Xu, J.; Kim, D. H.; Becerril, H. A.; Stoltenberg, R. M.; Lee, T. H.; Xue, G.; Mannsfeld, S. C. B. et al. Solution Coating of Large-Area Organic Semiconductor Thin Films with Aligned Single-Crystalline Domains. *Nat. Mater.* **2013**, *12*, 665–671.
- (23) Xiao, C.; Kan, X.; Liu, C.; Jiang, W.; Zhao, G.; Zhao, Q.; Zhang, L.; Hu, W.; Wang, Z.; Jiang, L. Controlled Formation of Large-Area Single-Crystalline TIPS-pentacene Arrays Through Superhydrophobic Micropillar Flow-Coating. *J. Mater. Chem. C* **2017**, *5*, 2702–2707.

- (24) Shao, Y.; Gan, Z.; Epifanovsky, E.; Gilbert, A. T.; Wormit, M.; Kussmann, J.; Lange, A. W.; Behn, A.; Deng, J.; Feng, X. et al. Advances in Molecular Quantum Chemistry Contained in the Q-Chem 4 Program Package. *Mol. Phys.* **2015**, *113*, 184–215.
- (25) Perdew, J. P.; Burke, K.; Ernzerhof, M. Generalized Gradient Approximation Made Simple. *Phys. Rev. Lett.* **1996**, *77*, 3865–3868.
- (26) Hehre, W. J.; Ditchfield, R.; Pople, J. A. Self-Consistent Molecular Orbital Methods. XII. Further Extensions of Gaussian-Type Basis Sets for Use in Molecular Orbital Studies of Organic Molecules. *J. Chem. Phys.* **1972**, *56*, 2257–2261.
- (27) Yeganeh, S.; Voorhis, T. V. Triplet Excitation Energy Transfer with Constrained Density Functional Theory. *J. Phys. Chem. C* **2010**, *114*, 20756–20763.
- (28) Pensack, R. D.; Tilley, A. J.; Parkin, S. R.; Lee, T. S.; Payne, M. M.; Gao, D.; Jahnke, A. A.; Oblinsky, D. G.; Li, P.-F.; Anthony, J. E. et al. Exciton Delocalization Drives Rapid Singlet Fission in Nanoparticles of Acene Derivatives. *J. Am. Chem. Soc.* **2015**, *137*, 6790–6803.
- (29) Jones, A. C.; Kearns, N. M.; Ho, J.-J.; Flach, J. T.; Zanni, M. T. Impact of Non-Equilibrium Molecular Packings on Singlet Fission in Microcrystals Observed using 2D White-Light Microscopy. *Nat. Chem.* **2020**, *12*, 40–47.
- (30) Jortner, J.; Rice, S. A.; Katz, J. L.; Choi, S. Triplet Excitons in Crystals of Aromatic Molecules. *J. Chem. Phys.* **1965**, *42*, 309–323.
- (31) Suna, A. Kinematics of Exciton-Exciton Annihilation in Molecular Crystals. *Phys. Rev. B* **1970**, *1*, 1716–1739.
- (32) Stuart, A. N.; Tapping, P. C.; Schreffl, E.; Huang, D. M.; Kee, T. W. Controlling the

- Efficiency of Singlet Fission in TIPS-Pentacene/Polymer Composite Nanoparticles. *J. Phys. Chem. C* **2019**, *123*, 5813–5825.
- (33) Tayebjee, M. J. Y.; Schwarz, K. N.; MacQueen, R. W.; Dvořák, M.; Lam, A. W. C.; Ghiggino, K. P.; McCamey, D. R.; Schmidt, T. W.; Conibeer, G. J. Morphological Evolution and Singlet Fission in Aqueous Suspensions of TIPS-Pentacene Nanoparticles. *J. Phys. Chem. C* **2016**, *120*, 157–165.
- (34) Lee, T. S.; Lin, Y. L.; Kim, H.; Pensack, R. D.; Rand, B. P.; Scholes, G. D. Triplet Energy Transfer Governs the Dissociation of the Correlated Triplet Pair in Exothermic Singlet Fission. *J. Phys. Chem. Lett.* **2018**, *9*, 4087–4095.
- (35) Pensack, R. D.; Ostroumov, E. E.; Tilley, A. J.; Mazza, S.; Grieco, C.; Thorley, K. J.; Asbury, J. B.; Seferos, D. S.; Anthony, J. E.; Scholes, G. D. Observation of Two Triplet-Pair Intermediates in Singlet Exciton Fission. *J. Phys. Chem. Lett.* **2016**, *7*, 2370–2375.
- (36) Lebental, M.; Choukri, H.; Chénais, S.; Forget, S.; Siove, A.; Geffroy, B.; Tutiš, E. Diffusion of Triplet Excitons in an Operational Organic Light-Emitting Diode. *Phys. Rev. B* **2009**, *79*, 165318.
- (37) Hertel, D.; Meerholz, K. Triplet-Polaron Quenching in Conjugated Polymers. *J. Phys. Chem. B* **2007**, *111*, 12075–12080.
- (38) Bayliss, S. L.; Thorley, K. J.; Anthony, J. E.; Bouchiat, H.; Greenham, N. C.; Chepelianskii, A. D. Localization Length Scales of Triplet Excitons in Singlet Fission Materials. *Phys. Rev. B* **2015**, *92*, 115432.
- (39) Gösele, U.; Seeger, A. Theory of Bimolecular Reaction Rates Limited by Anisotropic Diffusion. *Phil. Mag.* **1976**, *34*, 177–193.
- (40) Mozumder, A.; Pimblott, S. M. The Influence of the Diffusional Anisotropy on Bimolec-

- ular Reaction Rate of Neutrals in Molecular Crystals: Triplet–Triplet Annihilation in Anthracene. *Chem. Phys. Lett.* **1990**, *167*, 542–546.
- (41) Olaya-Castro, A.; Scholes, G. D. Energy Transfer from Förster–Dexter Theory to Quantum Coherent Light-Harvesting. *Int. Rev. Phys. Chem.* **2011**, *30*, 49–77.
- (42) Engel, E.; Leo, K.; Hoffmann, M. Ultrafast Relaxation and Exciton–Exciton Annihilation in PTCDA Thin Films at High Excitation Densities. *Chem. Phys.* **2006**, *325*, 170–177.
- (43) Marcus, R. A. On the Theory of Oxidation-Reduction Reactions Involving Electron Transfer. I. *J. Chem. Phys.* **1956**, *24*, 966–978.
- (44) Voter, A. F.; Doll, J. D. Transition State Theory Description of Surface Self-Diffusion: Comparison with Classical Trajectory Results. *J. Chem. Phys.* **1984**, *80*, 5832–5838.
- (45) Wan, Y.; Guo, Z.; Zhu, T.; Yan, S.; Johnson, J.; Huang, L. Cooperative Singlet and Triplet Exciton Transport in Tetracene Crystals Visualized by Ultrafast Microscopy. *Nat. Chem.* **2015**, *7*, 785–792.
- (46) Grieco, C.; Kennehan, E. R.; Kim, H.; Pensack, R. D.; Brigeman, A. N.; Rimshaw, A.; Payne, M. M.; Anthony, J. E.; Giebink, N. C.; Scholes, G. D. et al. Direct Observation of Correlated Triplet Pair Dynamics during Singlet Fission Using Ultrafast Mid-IR Spectroscopy. *J. Phys. Chem. C* **2018**, *122*, 2012–2022.
- (47) Grieco, C.; Doucette, G. S.; Munson, K. T.; Swartzfager, J. R.; Munro, J. M.; Anthony, J. E.; Dabo, I.; Asbury, J. B. Vibrational Probe of the Origin of Singlet Exciton Fission in TIPS-pentacene Solutions. *J. Chem. Phys.* **2019**, *151*, 154701.
- (48) Folie, B. D.; Haber, J. B.; Refaely-Abramson, S.; Neaton, J. B.; Ginsberg, N. S. Long-Lived Correlated Triplet Pairs in a π -Stacked Crystalline Pentacene Derivative. *J. Am. Chem. Soc.* **2018**, *140*, 2326–2335.

- (49) Hwang, D. K.; Fuentes-Hernandez, C.; Berrigan, J. D.; Fang, Y.; Kim, J.; Potscavage, W. J.; Cheun, H.; Sandhage, K. H.; Kippelen, B. Solvent and Polymer Matrix Effects on TIPS-pentacene/Polymer Blend Organic Field-Effect Transistors. *J. Mater. Chem.* **2012**, *22*, 5531–5537.
- (50) Ostroverkhova, O.; Shcherbyna, S.; Cooke, D. G.; Egerton, R. F.; Hegmann, F. A.; Tykwinski, R. R.; Parkin, S. R.; Anthony, J. E. Optical and Transient Photoconductive Properties of Pentacene and Functionalized Pentacene Thin Films: Dependence on Film Morphology. *J. Appl. Phys.* **2005**, *98*, 033701.
- (51) Pace, N. A.; Arias, D. H.; Granger, D. B.; Christensen, S.; Anthony, J. E.; Johnson, J. C. Dynamics of Singlet Fission and Electron Injection in Self-Assembled Acene Monolayers on Titanium Dioxide. *Chem. Sci.* **2018**, *9*, 3004–3013.
- (52) Sharifzadeh, S.; Wong, C. Y.; Wu, H.; Cotts, B. L.; Kronik, L.; Ginsberg, N. S.; Neaton, J. B. Relating the Physical Structure and Optoelectronic Function of Crystalline TIPS-Pentacene. *Adv. Funct. Mater.* **2015**, *25*, 2038–2046.
- (53) Ullah Khan, H.; Li, R.; Ren, Y.; Chen, L.; Payne, M. M.; Bhansali, U. S.; Smilgies, D.-M.; Anthony, J. E.; Amassian, A. Solvent Vapor Annealing in the Molecular Regime Drastically Improves Carrier Transport in Small-Molecule Thin-Film Transistors. *ACS Appl. Mater. Interfaces* **2013**, *5*, 2325–2330.
- (54) Yang, F.; Wang, X.; Fan, H.; Tang, Y.; Yang, J.; Yu, J. Effect of In Situ Annealing Treatment on the Mobility and Morphology of TIPS-Pentacene-Based Organic Field-Effect Transistors. *Nanoscale Res. Lett.* **2017**, *12*, 503.
- (55) Swenberg, C. E. Theory of Triplet Exciton Annihilation in Polyacene Crystals. *J. Chem. Phys.* **1969**, *51*, 1753–1764.
- (56) Bachilo, S. M.; Weisman, R. B. Determination of Triplet Quantum Yields from Triplet-Triplet Annihilation Fluorescence. *J. Phys. Chem. A* **2000**, *104*, 7711–7714.

- (57) Kondakov, D. Y.; Pawlik, T. D.; Hatwar, T. K.; Spindler, J. P. Triplet Annihilation Exceeding Spin Statistical Limit in Highly Efficient Fluorescent Organic Light-Emitting Diodes. *J. Appl. Phys.* **2009**, *106*, 124510.
- (58) Cheng, Y. Y.; Fückel, B.; Khoury, T.; Clady, R. G. C. R.; Tayebjee, M. J. Y.; Ekins-Daukes, N. J.; Crossley, M. J.; Schmidt, T. W. Kinetic Analysis of Photochemical Upconversion by Triplet Triplet Annihilation: Beyond Any Spin Statistical Limit. *J. Phys. Chem. Lett.* **2010**, *1*, 1795–1799.
- (59) Auckett, J. E.; Chen, Y. Y.; Khoury, T.; Clady, R. G. C. R.; Ekins-Daukes, N. J.; Crossley, M. J.; Schmidt, T. W. Efficient Up-Conversion by Triplet-Triplet Annihilation. *J. Phys. Conf. Ser.* **2009**, *185*, 012002.

TOC Graphic

